CrossMark

Responses of the zooplankton community to peak and waning periods of El Niño 2015–2016 in Kavaratti reef ecosystem, northern Indian Ocean

G. Vineetha · Kusum Komal Karati · T. V. Raveendran · K. K. Idrees Babu · C. Riyas ·
M. I. Muhsin · B. K. Shihab · Cheruvathoor Simson · P. Anil

Abstract The study addressed the impact of the El Niño 2015–2016 on the ecosystem functioning and the subsequent effects on the distribution and community structure of zooplankton in the Kavaratti reef, a prominent coral atoll in the tropical Indian Ocean. The elevated ocean temperature (SST) associated with El Niño resulted in a mass bleaching event affecting > 60% of the live corals of the Kavaratti atoll. The concomitant changes observed in the nutrient concentration, coral health, and phytoplankton of the reef environment during the course of the El Niño led to discernible variations in the zooplankton community with markedly higher abundance and heterogeneity in distribution during the peak period of El Niño compared to its waning phase. A notable shift was also evident in the community structure of Copepoda, the dominant zooplankton taxon, with a predominance of calanoids and poecilostomatoids in the peak period and by harpacticoid copepods in the waning phase of the El Niño. The harpacticoid, *Macrosetella gracilis*, dominated in the waning phase because of their unique adaptability in the utilization of *Trichodesmium erythraeum*, both as nutritional and physical substrates in the nutrient-depleted environment of the reef ecosystem.

G. Vineetha · K. K. Karati · T. V. Raveendran · P. Anil
National Institute of Oceanography-CSIR, Kochi 682018, India

K. K. Idrees Babu · C. Riyas · M. I. Muhsin · B. K. Shihab ·
C. Simson
Department of Science and Technology, Kavaratti, Lakshadweep
682555, India

Present Address:
G. Vineetha (✉)
Central Marine Fisheries Research Institute, Ernakulam North,
Kochi 682018, India
e-mail: vineetha.varada@gmail.com

Present Address:
K. K. Karati
Centre for Marine Living Resources & Ecology, Kochi 682037,
India

Introduction

Marine habitats ranging from shallow water reco-systems to deep ocean basins have a crucial role in sustaining the life on earth (Costello and Chaudhary 2017). The climate changes imposed by both natural and anthropogenic stresses severely affect the functioning and health of the marine habitats (Walther et al. 2002) The shallow water reef ecosystems bordering the tropical-subtropical belts are one such vulnerable oceanic habitats to the perils imposed by the climate variability (Baker et al. 2008). Alterations occurring in the physicochemical scenario of the reef habitats, like variations in the water pH and nutrient loads, elevated

Springer

sea surface temperature corresponding to global warming and temporary weather anomalies often threaten the functioning and biodiversity of the reef ecosystems (Diaz-Pulido et al. 2009).

El Niño Southern Oscillation (ENSO), an irregular interannual climate variability consisting of an alternating warm (El Niño) and cool (La Niña) oceanic episodes, is one such weather anomaly that brings about a sudden stress to the reef communities worldwide (Claar et al. 2018). Though it originates in the equatorial Pacific Ocean, its environmental impact is felt worldwide (McPhaden et al. 2006). The Lakshadweep group of islands in the Arabian Sea is one of the prominent coral reef ecosystems in the Indian subcontinent (James 2011). Similar to other reef ecosystems in the tropical and subtropical regions, the Lakshadweep coral atolls are very sensitive to the elevated SST associated with the recurrent El Niño climatic events (Arthur 2000). Hence, an extensive monitoring of the reef environment and associated biota is essential to manage the hazards induced by climatic variability and also for planning effective measures for the restoration of this valued ecosystem in the tropical Indian Ocean.

Zooplankton plays a pivotal role in the trophodynamics of reef ecosystems as an intermediary link between primary producers and higher trophic levels including the corals and reef-associated fishes (Heidelberg et al. 2010). Corals are polytrophic as they can ingest multiple food resources and rely on zooplankton for the nitrogenous and mineral requirements needed for their growth and reproduction (Houlbrèque et al. 2004). In the reef ecosystem, zooplankton species can be demersal, epibenthic, pelagic reef residents and offshore migrants. These aid them in the effective utilization of the diverse food resources in the reef ecosystem and in turn make them a suitable diet choice for a wide range of consumers in the food web (Madhupratap et al. 1991). Being extremely sensitive to subtle variations in its preferred habitat, zooplankton is often taken as an excellent ecological indicator of many physical processes and perturbations of climatic and anthropogenic origins (Richardson 2008). As evidenced in many studies, temperature, contingent to the tolerance limits and physiological responses of the zooplankton community, often has a determining role in shaping their abundance, phenology, and distribution patterns (Edwards and Richardson 2004; Hays et al. 2005). Hence, the unprecedented rise in temperature associated with El Niño events is anticipated to exert a profound influence on the abundance and community structure of the zooplankton in the reef ecosystems. As a major trophic resource of the reef corals and associated biota, the El Niño induced variability in the zooplankton abundance may reinforce the havoc brought about by the climatic event on the trophic ecology of the coral reef ecosystems. In view of this, a comprehensive evaluation of the spatiotemporal variations of diversity, distribution, and abundance of the zooplankton community in concurrence to the El Niño event is necessary to estimate the consequences brought about this interannual climatic variability on the trophic ecology and functioning of the coral reef ecosystems. In spite of the researchers tackling El Niño impacts on corals (Arthur 2000; Glynn et al. 2017), primary producers and top predators of the reef ecosystem (Wilson et al. 2001; Bakun and Broad 2003), studies related to its impact on the reef-associated zooplankton community are often neglected. Though many studies have focussed on the diversity and distribution of zooplankton in the Lakshadweep reef ecosystem (Achuthankutty et al. 1989; Madhupratap et al. 1991), the perturbations generated by the climatic event on this important plankton component remain hitherto unaddressed.

It is hypothesized that the El Niño-induced changes in the hydrographic characteristics and biotic components (phytoplankton and coral communities) will enunciate varied responses among the diverse zooplankton taxa depending on their species-specific traits and in turn will have a crucial influence on the reef ecosystem functioning. Based on the satellite observations and in situ cruise data, the occurrence of a strong El Niño was observed for the period from late 2015 to early 2016 in the tropical Pacific Ocean (Stramma et al. 2016). Taking into consideration both the intensity of this El Niño event and the scarcity of our knowledge on the response of the zooplankton community to this climatic phenomenon, the present study was designed to evaluate the responses of the zooplankton community to the variability generated in the reef habitat during the El Niño 2015–2016.

Materials and methods

Study area

Kavaratti atoll lies in the Lakshadweep group of islands in the northern Indian Ocean. A total of 12

atolls encompassing 27 small islands and having a total land area of 32 km^2 comprises the Lakshadweep archipelago (8°–12° N and 71°–74° E). Kavaratti, located at about 400 km distance from the mainland of India, is one of the prominent atolls in this island group. The lagoon is 4500 m long and hosts a rich coral and fish diversity (Arthur 2000; Vijay Anand and Pillai 2007).

Sampling

To evaluate the hydrographic characteristics and the biotic community of the Kavaratti atoll, sampling was done at ten sites covering the entire lagoon (Fig. 1). Giving emphasis to the varied nature of the lagoon substratum, four sampling stations (St 3, 5, 8, and 10) were fixed at regions where corals were present whereas the remaining six stations (St 1, 2, 4, 6, 7, and 9) were set in areas characterized by sandy substratum (Fig. 1). As the primary aim of the study was to assess the impact of El Niño on the zooplankton community, the sampling period was fixed based on the El Niño forecast of the Earth Institute, Colorado University (http://iri.columbia.

edu/ourexpertise/climate/forecasts/enso/2016). The first sampling was done during the El Niño peak phase (first week of March 2016) whereas the second sampling was carried out in its waning phase (last week of May 2016). To have a detail perception on the influence of this climatic event on the SST around the Lakshadweep archipelago, the satellite-based SST of the Lakshadweep Sea in the vicinity of the coral atolls (8° N–12° N and 71° E–74° E) was computed (monthly composite) for the last ENSO cycle of 2010–2016. The ENSO cycle was determined following the Oceanic Niño Index, the de-facto standard used to monitor the El Niño Southern Oscillation (http://ggweather.com/enso/oni.htm) in the tropical Pacific Ocean, covering the La Niña year 2010–2011, neutral years 2011–2015, and El Niño year 2015–2016. The necessary SST data for the period of the ENSO cycle was extracted from the GAC in NOAA Ocean Watch LAS (Jun 2010–Dec 2015) and MODISA_L3m_SST (Jan 2016–May 2016). Concurrent to the satellite retrieval, the in situ SST of the sampling locations inside the lagoon during both the sampling periods were monitored using a bucket thermometer.

Fig. 1 Sampling locations in the Kavaratti lagoon in the northern Indian Ocean
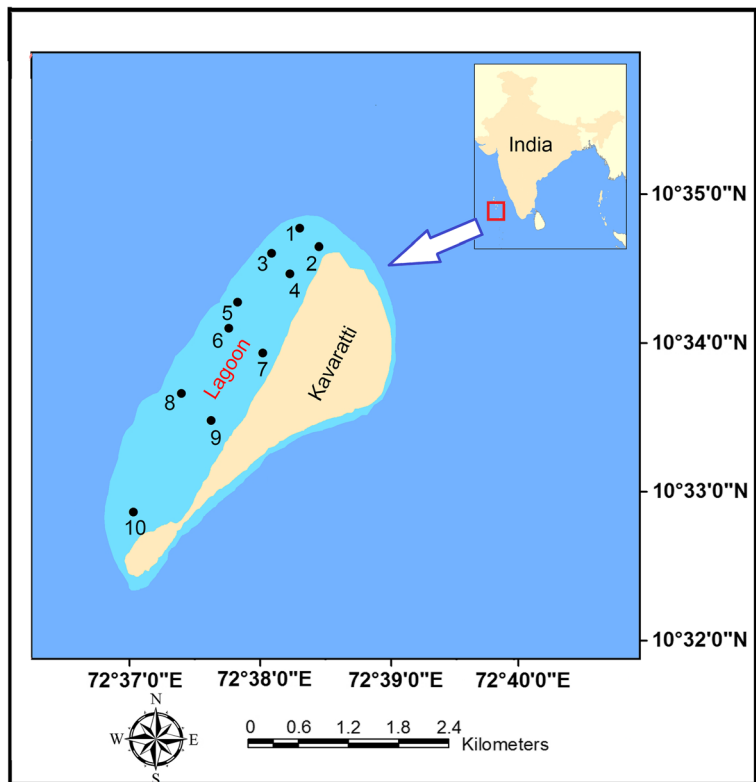
For determining the hydrographic characteristics of the reef water and also the phytoplankton community, surface water samples were collected using a Niskin sampler (5 l capacity). The surface salinity of the reef waters was measured using an Autosal (DIGI-AUTO Model-5, accuracy ± 0.005) whereas the pH was estimated using a calibrated pH meter (ELICO LI610, accuracy ± 0.01). Nutrients (nitrate, nitrite, ammonium, phosphate, and silicate) were analyzed following the standard colorimetric techniques (Grasshoff 1983), using an Auto Analyzer (SKALAR San++ System, Netherland). The precision of nutrient measurements was ± 0.15 μmol N l^{-1} for nitrate, ± 0.04 μmol P l^{-1} for phosphate, and ± 0.05 μmol Si l^{-1} for silicate respectively. For the estimation of the size-fractionated phytoplankton biomass (chlorophyll a), 2 l of the surface water samples was collected using Niskin sampler for the sequential filtration procedure. The water samples were first passed through a 200-μm mesh and concurrently through a 20-μm mesh for the biomass estimation of the macro- and microplankton respectively. Subsequent to the filtration process, the water samples were again re-filtered through 2- and 0.2-μm polycarbonate filters for the biomass estimation of the nano- and picophytoplankton fractions respectively. After the sequential filtration process, the pigment extraction of all the size classes was carried out using 90% acetone at 4 °C for 24 h in the dark, and the respective concentration was estimated fluorometrically (Turner Designs, 7200) (Parsons 1984). For the phytoplankton species identification, 2 l of the surface water samples was fixed immediately with 1% acid Lugol's iodine and after the settling and siphoning procedure, the phytoplankton species were identified and enumerated under a binocular inverted microscope (OLYMPUS, CK-30) in a Sedgewick-Rafter counting chamber following the standard identification protocols (Tomas 1997).

Zooplankton samples were collected using a Working Party net-2 (mesh size 200 μm) with a mouth area of 0.28 m^2. The net was towed horizontally just below the surface for 10 min at a consistent speed (~ 1 knot) to minimize the net avoidance by the larger zooplankton. A digital flowmeter (Hydro-Bios, Model 438110) was attached across the mouth of the net to estimate the amount of water filtered. After the collection, the zooplankton samples were passed through 200-μm net, excess water removed using an absorbent paper, and the biomass estimated following the displacement volume method (Hagen 2000). The samples were immediately preserved in 4% formaldehyde solution (Harris et al. 2000), and zooplankton was sorted into groups, identified, and their abundance estimated and expressed as individuals/cubic meter (ind m^{-3}). The species-level identification of the dominant taxon, Copepoda, was carried out following the standard identification keys (Sewell 1999; Conway et al. 2003).

Reef corals being the fundamental community in the reef ecosystem whose growth and vigor have a vital influence on the ecosystem functioning, the line intercept transect (LIT) method was carried out during October 2015 and May 2016, to have a better perception of the reef status and the coral percentage cover in the lagoon (Loya 1972). The transects were laid horizontally along the substratum, and the status of the reef coral was evaluated along each transect. The projected length of each substrate category or coral species beneath the 50 m line was recorded to the nearest centimeter. The live corals were identified to genus and/or species level and the periodic changes occurring in the substrate type were recorded. Percentage of coral cover in the Kavaratti atoll was monitored by snorkeling and scuba diving. Taxonomic identification of the corals was carried out following the Indo Pacific Coral Finder robust underwater plastic book (Kelley 2009).

Statistical analyses

To have a better understanding of the significance of variation existing between the two sampling periods, a paired t test (parametric or non-parametric Wilcoxon test) with two-tailed P values and 95% confidence intervals was performed for the abiotic variables. The parametric or non-parametric t test was determined based on the D'Agostino and Pearson omnibus normality test of the dataset. Similarly, the paired t test was performed on the biomass and abundance of both phytoplankton and zooplankton communities. The correlation analysis was performed between the zooplankton abundance and the various size-structured phytoplankton biomasses to assess their interrelation.

Non-metric multidimensional scaling (NMDS) was carried out based on the abundance of various zooplankton taxa of the sampling locations to assess the distinctness in the community structure between the two sampling periods using PRIMER (Clarke and Gorley 2015). NMDS helps to visualize the data points in a two-dimensional plane so that highly similar sets are plotted

close together. Hence, the analysis was further done for the dominant zooplankton taxon, Copepoda, based on the Bray-Curtis similarity index (Clifford and Stephensen 1975) applied on the fourth root transformed abundance of the copepod species.

The analysis of similarity (one-way ANOSIM) was carried out to describe (dis)-similarities of the zooplankton community between the two sampling phases using PRIMER (Clarke and Gorley 2015). The analysis was further done in the copepod community to identify the (dis)-similarities of the copepod community to get a better precision of the zooplankton community structure between the two periods. Also, the community indices, i.e., species diversity (H') and evenness (J') were analyzed to assess the spatiotemporal variation in the copepod species diversity and distribution pattern.

Along with the community indices, the ranked species abundance curves, which rank the species in terms of the decreasing order of their abundance, aid to provide a better understanding of the species dominance and diversity in an ecosystem (Warwick et al. 2008). Hence, the k-dominance curve was plotted using the copepod species abundance of both the sampling periods. Additionally, the characterizing copepod species of each sampling period were identified using SIMPER analysis based on their fourth root transformed abundance (Clarke and Gorley 2015).

The redundancy analysis (RDA), which explains the linear relationships existing between the response variables and explanatory variables, was used to understand the interrelation of the zooplankton taxa (response variables) with other biotic and abiotic variables during both the sampling periods (Van den Wollenberg 1977). The RDA was further carried out to identify the interrelation existing between the copepod species (response variables) and the phytoplankton community (explanatory variables).

Results

Hydrography

The monthly mean SST of the Lakshadweep Sea around the coral atolls exhibited a negative anomaly during the moderate La Niña year (2010–2011) and positive anomaly during the current El Niño year (2015–2016) (Fig. 2). In the in situ observation, during the peak phase of El Niño (first week of March 2016; winter monsoon), the SST varied between 30 and 31.4 °C (av. 30.6 ± 0.5 °C; Fig. 3a) and in the waning phase (fourth week of May 2016; late spring intermonsoon), it ranged between 30.6 and 31.7 °C (av. 31.1 ± 0.4 °C; Fig. 3b). The seasonal interference on the temperature was evident as in both in situ and satellite observations, the SST was

Fig. 2 SST anomaly of the Lakshadweep Sea, in the vicinity of the coral atolls (8° N to 12° N and 71° E to 74° E) during the moderate La Niña year –2011 and El Niño year 2015–2016
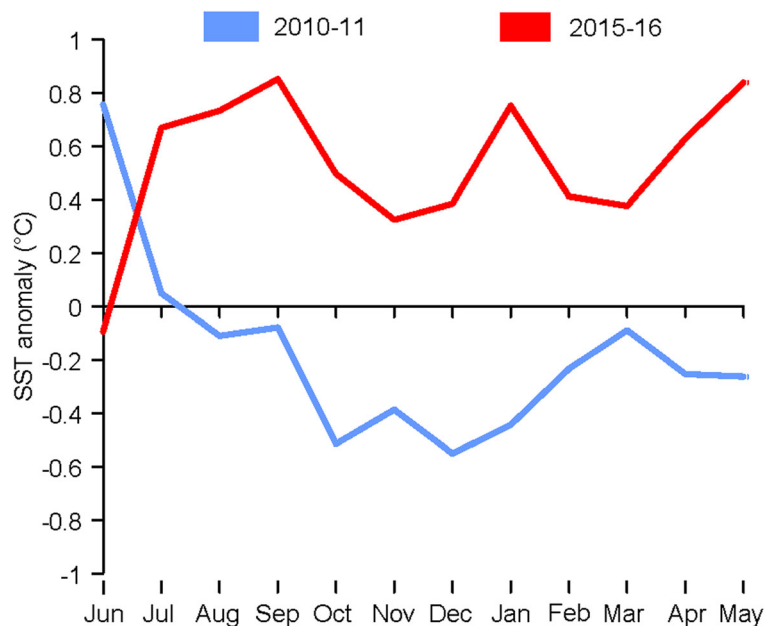
relatively high during waning phase with significant variation ($P < 0.05$). The surface salinity showed less spatial variation during both peak and waning phases (Fig. 3b). However, along with a temporal scale, the salinity was relatively high during waning phase (av. 34.79 ± 0.03, range 34.7–34.8) compared to the peak phase (av. 34.53 ± 0.09, range 34.4–34.7).

Nutrients

Although the reef was oligotrophic during both phases of the El Niño event, a temporal variation was observed in the nutrient concentration in the lagoon water. The peak phase nitrate concentration (av. 0.46 ± 0.52 μM) was 2.9 times higher than the waning phase (av. 0.16 ± 0.13 μM), and the variation was statistically significant ($P < 0.05$) (Fig. 4a). In the case of nitrite also, the peak phase concentration (av. 0.22 ± 0.06 μM) was significantly higher (2.4 times, $P < 0.05$) than the waning phase (av. 0.09 ± 0.03 μM) (Fig. 4b). Compared to the other nitrogenous sources, the concentration of ammonium was higher in the reef water during both the peak (av. 8.7 ± 1 μM) and waning phases (av. 5.4 ± 0.4 μM) (Fig. 4c). In accordance with the nitrogenous nutrients, the other essential nutrients, phosphate, and silicate also exhibited a similar mode in their temporal distribution. During the peak phase, the phosphate (av. 0.26 ± 0.15 μM) concentration was observed to be twice higher than that observed during the waning period (av. 0.13 ± 0.3 μM) (Fig. 4d). Similarly, the silicate concentration during peak phase (av. 4.7 ± 0.8 μM) was ~ 3 times higher than that of the waning phase (av. 1.59 ± 0.2 μM) ($P < 0.05$) (Fig. 4e).

Coral community

Taxonomically, a total of 23 genera of corals were identified in the lagoon (Table 1). Based on the line intercept transect method, massive hermatypic coral *Porites* sp. was found to be the dominant genus (22.41%). The other abundant (> 5%) genera were *Pocillopora*, *Oulophyllia*, *Lobophyllia*, and *Pavona*. The coral community of Kavaratti atoll experienced severe bleaching, meaning a rapid loss of pigmentation eventually leading to whitening of coral colony concurrent with the unprecedented rise in the SST with the El Niño event. More than 60% of the corals experienced bleaching during May 2016, and both fast-growing (*Acropora* spp.) and slower growing corals (*Porites* spp.) were severely affected. This led to a marked difference in the percentage of both live and dead coral covers in the lagoon. The live corals' cover of the pre-bleaching period (October 2015) of the lagoon (21.34%) drastically decreased to 9.89% during the waning phase of the El Niño (May 2016). In contrast, the dead and near dead coral reef area cover of the lagoon increased from 45.96% (only dead corals, pre-bleaching period) to 57.3% (50.7% dead +6.6% pale colored weak).

Phytoplankton biomass and abundance

Prominent spatiotemporal variation was observed in the phytoplankton biomass (chlorophyll *a*) and abundance (Fig. 5a, b). The total chlorophyll *a* during the peak El Niño phase (av. 0.17 ± 0.11 mg m^{-3}) dropped significantly ($P < 0.05$) in the waning phase (av.
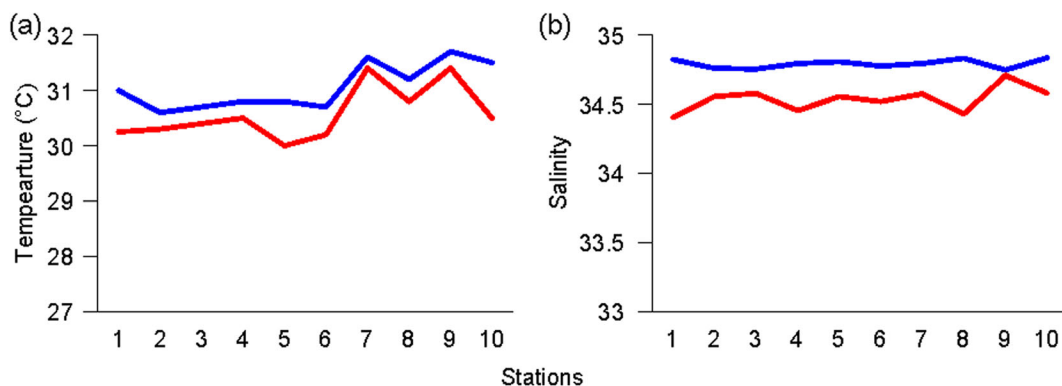

Fig. 3 Spatial distribution of **a** temperature (°C) and **b** salinity at the surface water of Kavaratti lagoon during the peak (red color) and waning phases (blue color) of El Niño
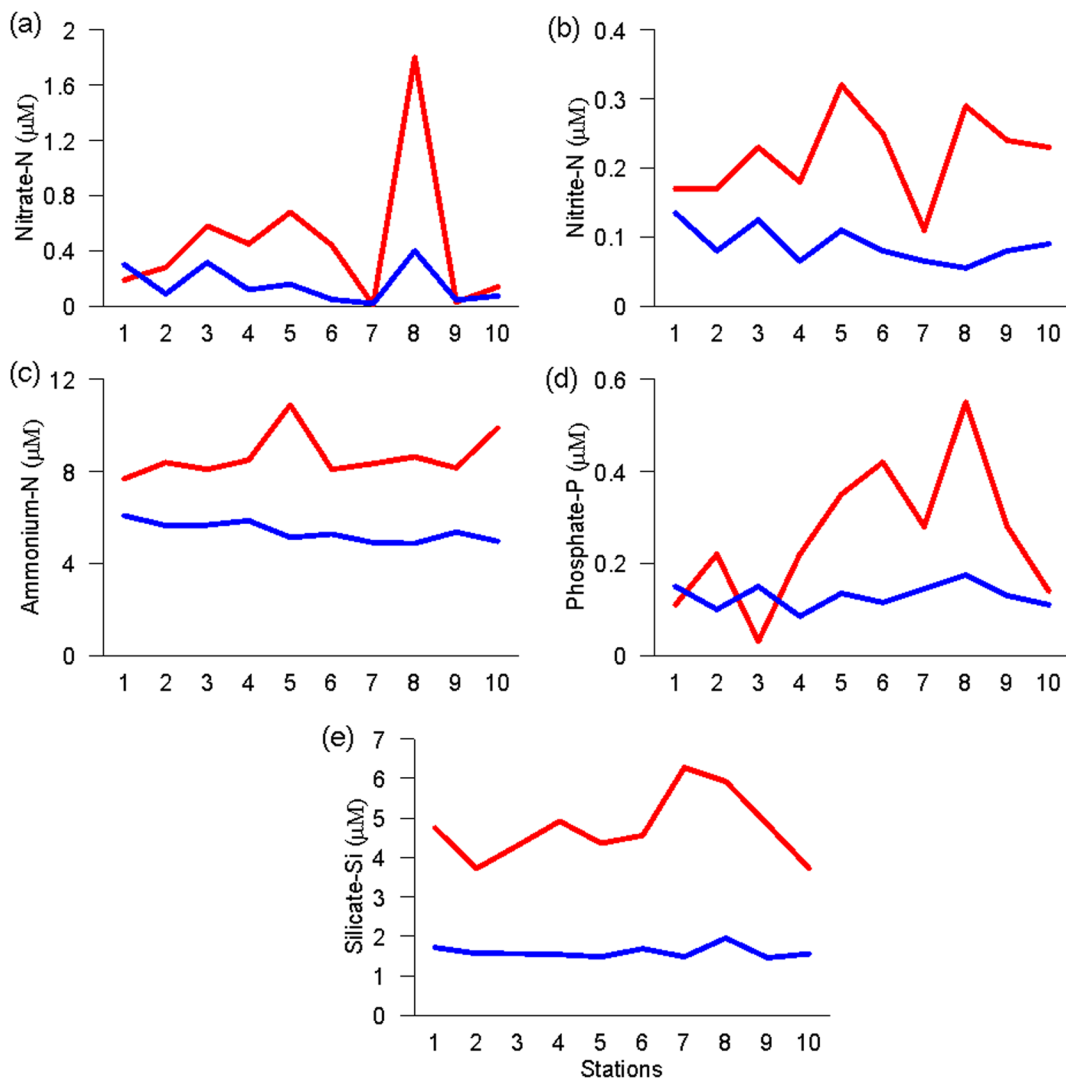
Fig. 4 a–e Spatial distribution of nutrients in the Kavaratti lagoon during the peak (red color) and waning phases (blue color) of El Niño

0.095 ± 0.04 mg m^{-3}). Considering the size-fractionated phytoplankton biomass distribution, all the size groups of the phytoplankton community except macroplankton exhibited higher biomass during the peak phase (Fig. 5a). Irrespective of the sampling periods, the nanophytoplankton contributed a major share of the phytoplankton biomass with 69.9 and 57.2%, during the peak and waning phases, respectively. The microphytoplankton also had a notable contribution towards the phytoplankton biomass during both the sampling periods (16.6 and 21.5%, in the peak and waning phases, respectively). In the case of the contribution by the picophytoplankton, not much variation was evident between the peak (10.6%) and waning

phases (12.4%). Interestingly, the macrophytoplankton which shared a minor percentage of the biomass in the peak phase (2.9%) contributed a good share (8.4%) to the phytoplankton biomass in the waning phase of the El Niño event (Fig. 5a). The phytoplankton abundance during the waning phase (1408 ± 802 cells l^{-1}) was significantly lower ($P < 0.05$) than the peak phase (3968 ± 2540 cells l^{-1}).

A notable change was also observed in the contribution of the different phytoplankton functional groups between the two sampling periods. In the peak phase, dinoflagellate (56.5%) formed the major contributor to the phytoplankton population followed by the diatoms (36.3%) and the higher abundance of

Table 1 Percentage contribution of coral genera in the Kavaratti atoll

Genus	Percent
Acropora	2.1
Montipora	1.3
Astreopora	0.9
Fungia	0.39
Cyphastrea	0.8
Favites	0.4
Favia	4.6
Galaxea	0.2
Gardineroseris	0.5
Goniastrea	1.13
Hydnophora	4.6
Leptastrea	3.16
Oulophyllia	12.45
Lobophyllia	8.47
Pachyseris	0.7
Pavona	6.25
Platygyra	1.96
Plesiastrea	0.3
Pocillopora	19.37
Porites	22.41
Psammocora	2.92
Symphyllia	4.8
Trachyphyllia	0.3

Prorocentrum lima at stations 7 and 9 had an important contribution in the higher abundance of dinoflagellates. In the waning phase, diatom formed the dominant group (54.5%) and a remarkable drop was noticed in the percentage contribution of the dinoflagellates (8.2%). Another noteworthy feature observed in the waning phase was the predominance of the blue-green algae, contributing 33.2% of the phytoplankton population (Table 2). The blue-green algae, *Trichodesmium erythraeum*, which had contributed only 2.4% of the total phytoplankton population during peak phase, occurred throughout the sampling locations in the waning phase and became predominant (33.2%) to the total phytoplankton population. *Thalassiosira* sp., *Diploneis* sp., *Prorocentrum lima*, and *Protoperidinium* sp. were the dominant species during the peak phase. Except for *T. erythraeum*, the abundant species in the waning phase were *Navicula delicatula* (24.4%) and *Licmophora abbreviata* (9.7%).

Zooplankton biomass and abundance

The zooplankton biomass and abundance exhibited both spatial and temporal variations in the study region (Fig. 5c, d). In the peak El Niño phase, zooplankton biomass ranged between 0.009 and 0.2 ml m^{-3} (av. 0.05 ± 0.06 ml m^{-3}), while the abundance ranged between 38 and 1042 ind m^{-3} (av. 288 ± 314 ind m^{-3}) (Fig. 5c). In the corresponding waning phase, both the biomass and the abundance dropped throughout the sampling locations (except station 2) with a significant statistical variation ($P < 0.05$) (Fig. 5c, d). The biomass in the waning phase varied between 0.006 and 0.04 ml m^{-3} (av. 0.02 ± 0.01 ml m^{-3}) whereas the abundance ranged between 26 and 201 ind m^{-3} (av. 108 ± 59 ind m^{-3}). However, spatially both the biomass and abundance were high at sampling stations characterized by live coral cover (biomass 0.09 ± 0.08 and 0.03 ± 0.02 ml m^{-3}, abundance 414 ± 441 and 132 ± 73 ind m^{-3}, during peak and waning phases, respectively) compared to other locations with predominant sandy bottom (biomass 0.03 ± 0.03 and 0.02 ± 0.01 ml m^{-3}, abundance 205 ± 199 and 92 ± 48 ind m^{-3} during peak and waning periods, respectively). In the waning phase, though a significant drop in zooplankton biomass and abundance was evident in sampling sites characterized by coral and sandy substratum, the variation was more conspicuous in regions where the coral community predominated (Fig. 5c, d).

Zooplankton composition and distribution

A total of 21 zooplankton taxa were observed during the study period among which Copepoda dominated contributing 94 and 93.5% of the total zooplankton population during the peak and waning phases. Though the number of taxa observed did not vary between two phases (18 each), there was an evident change in the community composition, abundance, and relative contribution to the total zooplankton population (Table 3). During peak phase, except copepod, the other abundant taxa (> 1% of the total zooplankton population) were Copelata, decapod larvae, and barnacle larvae, and in the case of waning phase, the other abundant taxon was bivalve larvae (Table 3). The carnivorous taxon Chaetognatha was present in all the station locations during both phases but had 10.6 times higher abundance in the peak phase. Except for Chaetognatha, the other exclusively carnivorous gelatinous taxa like
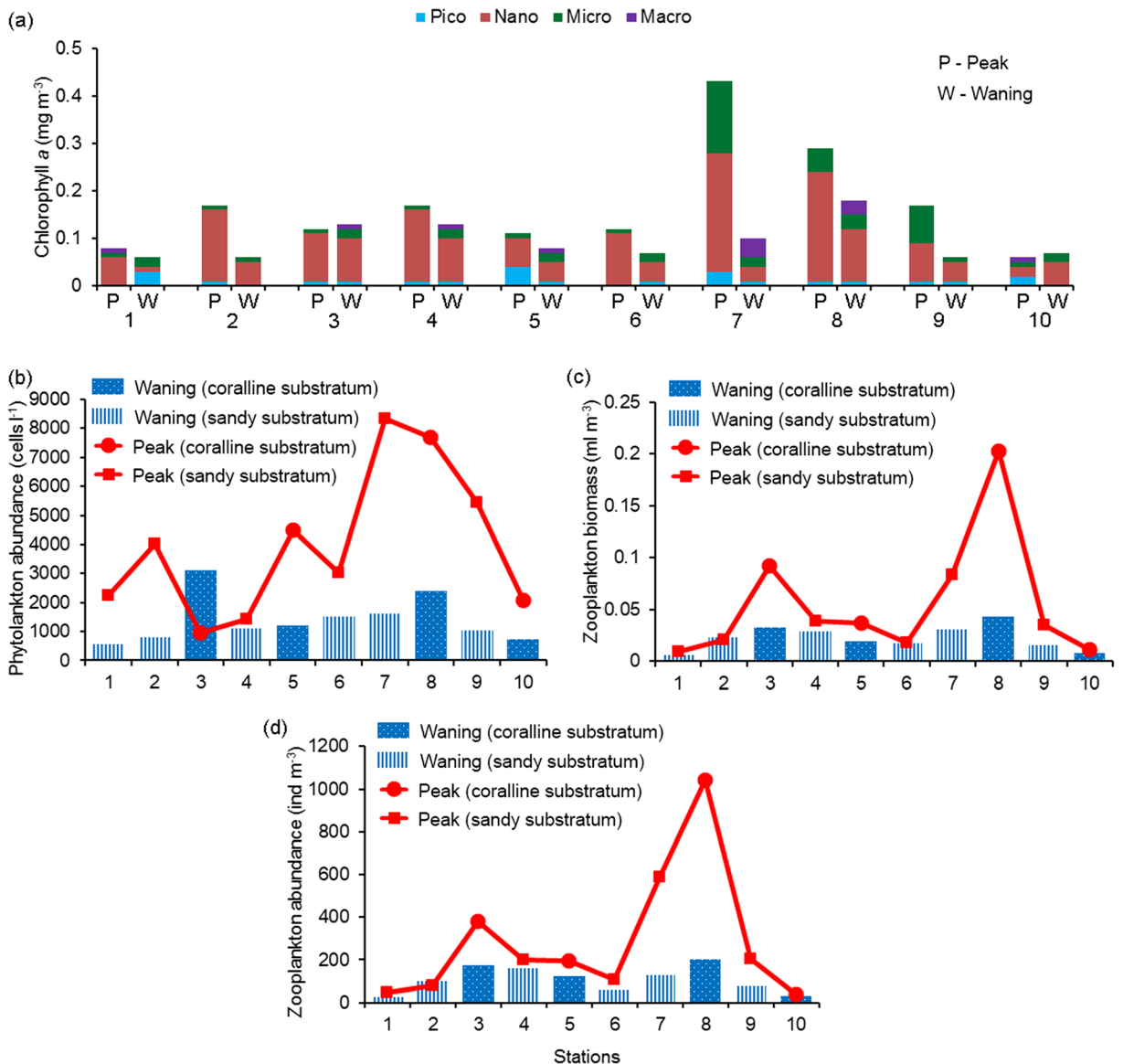
Fig. 5 Distribution of **a** size-fractionated chlorophyll *a* (mg m^{-3}), **b** phytoplankton abundance (cells l^{-1}), **c** zooplankton biomass (ml m^{-3}), and **d** zooplankton abundance (ind m^{-3}) in the Kavaratti lagoon during the peak and waning phases of El Niño. For biotic variables, different shapes were used for the coralline and sandy substratum (**b**–**d**)

Hydromedusae and Siphonophora also had relatively higher abundance in the peak phase compared to the waning phase (Table 3). The economically important meroplanktonic groups, especially decapod larvae, fish egg, and fish larvae, had markedly higher abundance in the peak phase compared to the waning phase (10.8, 10.9, and 353.6 times greater for decapod larvae, fish egg, and fish larvae, respectively).

Copepoda composition and distribution

A total of 60 copepod species belonging to orders Calanoida, Cyclopoida, Poecilostomatoida, and Harpacticoida were observed in the study region during the two sampling periods. Similar to the phytoplankton community, though the number of copepod species found in the peak (56) and waning phases (50) did not differ much, a conspicuous variation was evident in the

Table 2 Percentage contribution of the phytoplankton species during the peak and waning phases of El Niño (+ indicates < 1%, ++ indicates 1–5%, +++ indicates 5–10%, ++++ indicates > 10–20%, +++++ indicates > 20%)

Species	Peak	Waning
Thalassiosira sp.	++	++
Thalassiosira subtilis	+	−
Leptocylindrus danicus	−	++
Bacteriastrum furcatum	−	+
Chaetoceros sp.	−	+
Odontella mobiliensis	+++	+
Fragilaria crotonensis	++	+
Asterionellopsis glacialis	−	+
Pleurosigma sp.	++	++
Pleurosigma normanii	−	+
Pleurosigma elongatum	−	++
Gyrosigma sp.	+	++
Diploneis sp.	+++	++
Diploneis smithii	++	−
Diploneis didyma	+	−
Diploneis puella	+	−
Navicula sp.	+	++
Navicula delicatula	++	+++++
Mastogloia sp.	+	+
Mastogloia linearis	+	−
Entomoneis sp.	−	+
Amphora obtusa	+	−
Licmophora abbreviata	++	+++
Cylindrotheca closterium	−	++
Surirella fastuosa	−	+
Paralia sulcata	−	+
Prorocentrum lima	+++++	++
Prorocentrum rhathymum	+	−
Prorocentrum compressum	++++	+
Gyrodinium sp.	++	−
Ceratium declinatum	+	−
Diplopsalis sp.	++	++
Protoperidinium sp.	+++	++
Protoperidinium quinquecorne	++	−
Trichodesmium erythraeum	++	+++++
Dictyocha fibula	−	+
Unidentified	++	+

Table 3 Abundance of the zooplankton taxa during the peak and waning phases of El Niño

Zooplankton taxa	Peak	Waning
Chaetognatha	1.29 ± 1.4	0.12 ± 0.09
Hydromedusae	0.006 ± 0.02	0
Siphonophora	0.023 ± 0.07	0.002 ± 0.006
Doliolida	0.022 ± 0.07	0
Copelata	2.81 ± 2.83	0.14 ± 0.27
Copepoda	271 ± 295	101 ± 57
Amphipoda	0.006 ± 0.02	0.061 ± 0.08
Ostracoda	0	0.006 ± 0.02
Stomatopoda	0.023 ± 0.07	0.005 ± 0.008
Lucifer	0.007 ± 0.01	0.014 ± 0.02
Cephalopoda	0.001 ± 0.002	0.002 ± 0.006
Cladocera	0.273 ± 0.34	0.179 ± 0.29
Foraminifera	0.51 ± 0.8	0.12 ± 1.2
Decapoda larvae	6.5 ± 6.85	0.6 ± 0.9
Gastropoda larvae	0.756 ± 1.1	0.758 ± 0.78
Bivalve larvae	0.48 ± 0.7	3.38 ± 4.25
Polychaete larvae	0.016 ± 0.03	0.011 ± 0.01
Barnacle larvae	2.99 ± 8.93	0.19 ± 0.34
Echinoderm larvae	0	0.01 ± 0.03
Fish egg	1.01 ± 1.35	0.09 ± 0.11
Fish larvae	0.561 ± 1.05	0.002 ± 0.005

community composition, abundance, and percentage contribution between the two sampling periods (Table 4). Though calanoids dominated the copepod community during both the periods, their percentage contribution was relatively high in the peak phase (62 and 48% during peak and waning phases, respectively). Contrastingly, the harpacticoids which shared a minor percentage of the copepod population in the peak phase (1.3%) had a considerably higher contribution in the waning phase (19.7%) (Table 4). *Bestiolina similis*, *Acrocalanus gracilis*, and *Oncaea venusta* remained the dominant species (based on dominancy analysis) throughout the study period. Of the other copepod species observed during the study, *Acartia dweepi*, *Oithona plumifera*, and *Oithona brevicornis* predominated during the peak phase, whereas *Paracalanus aculeatus*, *Calanopia minor*, *Corycaeus speciosus*, and *Macrosetella gracilis* formed the dominant species of the waning phase. Although majority of the copepod species exhibited lower abundance in the waning phase, copepods belonging to the order Harpacticoida and most prominently the species *Macrosetella gracilis* had relatively high abundance in the waning phase of the El Niño event (Table 4).

Table 4 Abundance of the copepod species during the peak and waning phases of El Niño (* indicates < 0.01, ** indicates 0.01–0.1, *** indicates > 0.1–1, **** indicates > 1–10, ***** indicates > 10 ind m^{-3})

Copepod species	Peak	Waning
Undinula vulgaris	****	****
Canthocalanus pauper	*****	****
Cosmocalanus darwinii	****	***
Bestiolina similis	*****	*****
Paracalanus aculeatus	*****	****
Acrocalanus gracilis	*****	****
Acrocalanus monachus	****	*
Subeucalanus subcrassus	****	***
Subeucalanus mucronatus	***	—
Acartia erythraea	***	—
Acartia danae	****	****
Acartia dweepi	*****	***
Acartia amboinensis	****	***
Acartia spinicauda	**	—
Temora discaudata	****	***
Euchaeta rimana	****	****
Euchaeta marina	**	**
Euchaeta longicornis	*	—
Centropages gracilis	***	***
Centropages furcatus	****	***
Centropages orsini	****	****
Centropages calaninus	***	****
Labidocera pectinata	**	**
Labidocera detruncata	***	*
Labidocera pavo	*	***
Labidocera sp.	***	—
Pontellina plumata	***	**
Pontellopsis spp.	***	—
Calanopia minor	***	****
Candacia bradyi	**	***
Candacia catula	****	****
Candacia curta	****	***
Candacia discaudata	*	—
Lucicutia flavicornis	**	**
Oithona plumifera	*****	****
Oithona brevicornis	*****	****
Oithona similis	****	****
Oncaea media	****	****
Oncaea venusta	*****	****
Oncaea conifera	****	***
Oncaea mediterranea	****	****
Corycaeus speciosus	*****	****

Table 4 (continued)

| Copepod species	Peak	Waning
Onychocorycaeus agilis	****	***
Monocorycaeus robustus	****	—
Urocorycaeus longistylis	****	****
Onychocorycaeus catus	****	***
Urocorycaeus latus	***	*
Ditrichocorycaeus asiaticus	***	***
Corycaeus vitreus	***	—
Copilia mirabilis	***	**
Sapphirina ovatolanceolata	—	*
Sapphirina angusta	****	—
Sapphirina sp.	**	**
Farranula gibbula	****	****
Macrosetella gracilis	***	*****
Microsetella norvegica	****	****
Euterpina acutifrons	—	****
Clytemnestra scutellata	****	**
Metis jousseaumei	—	***
Longipedia sp.	—	**
Unidentified copepodite	****	****

Data analyses

NMDS

A marked difference in the position of the sampling locations between the peak and waning phases was observed in the NMDS plot based on the Bray-Curtis similarity indices using the abundance of the zooplankton taxa (stress 0.17, Fig. 6). The NMDS plot based on the abundance data of the copepod species also exhibited a similar scenario to that of the zooplankton community (stress 0.17).

Analysis of similarity

The analysis of similarity indicated a significantly distinguishable zooplankton community in the peak phase from that of the waning phase (one-way ANOSIM, global $R = 0.395$, $P = 0.001$). The result of this statistical analysis based on the copepod species abundance also exhibited a similar output (global $R = 0.405$, $P = 0.001$).

Fig. 6 Non-metric multidimensional scaling (NMDS) plot of sampling locations based on the abundance of **a** zooplankton taxa and **b** copepod species
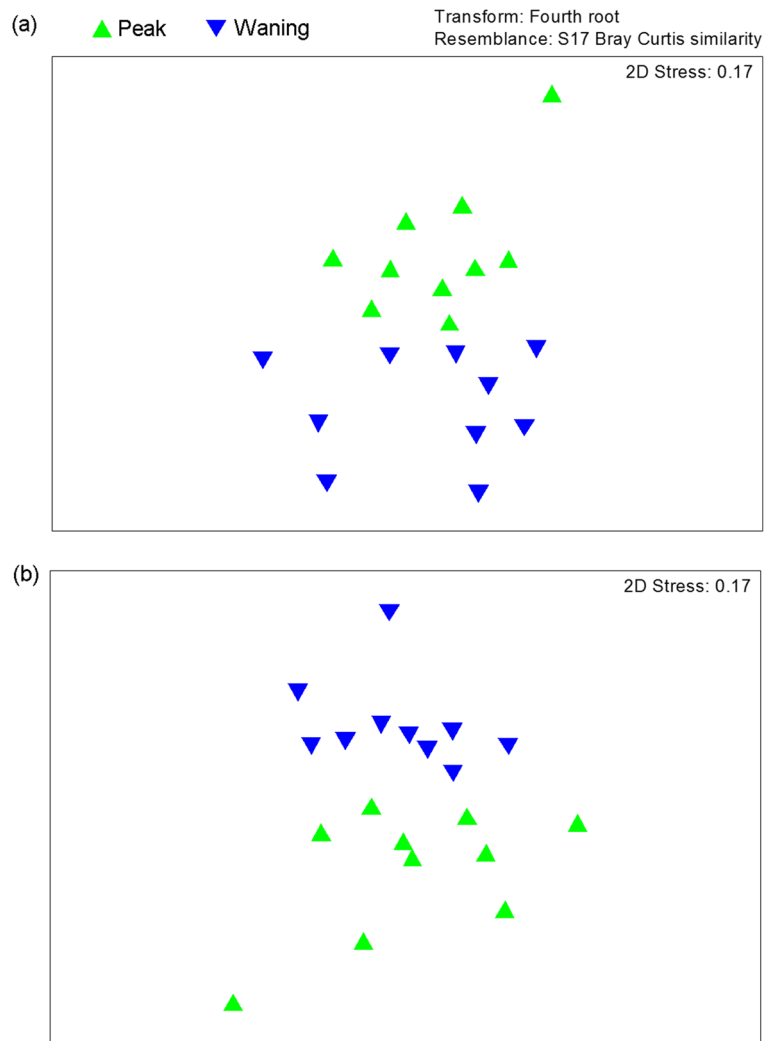
Community indices

Although copepod species composition and their abundance exhibited a conspicuous variation between the two sampling phases, no significant variation ($P > 0.05$) was observed in the species diversity (H') (Fig. 7). However, a marked spatial variation was evident in the H' during the peak phase, as it ranged between 1.84 and 4.44 (av. 3.72 ± 0.75), whereas in the waning phase, the spatial variation in diversity was negligible (range, 3.13–4.2; av. 3.89 ± 0.33). Similar to H', species evenness (J') also did not show significant temporal variation ($P > 0.05$). In the peak phase, J' varied between 0.53 and 0.89 (av. 0.79 ± 0.1) whereas during waning phase, it ranged between 0.76 and 0.89 (0.84 ± 0.03) (Fig. 7).

Dominance index

In the case of the k-dominance plot, it was observed that both the maximum and minimum diversities of species were observed during the peak phase indicating towards heterogeneity in the spatial distribution of copepod (Fig. 8). Contrastingly, in the waning phase, the dominance curve exhibited less variation.

Similarity percentage routine analysis

The similarity percentage routine (SIMPER) analysis helped to identify the characterizing and discriminating species of Copepoda during both the peak and waning phases. The average similarity observed for the Copepoda species was relatively low in the peak phase

Fig. 7 **a** Species diversity (H') and **b** species evenness of Copepoda (J') along the sampling locations
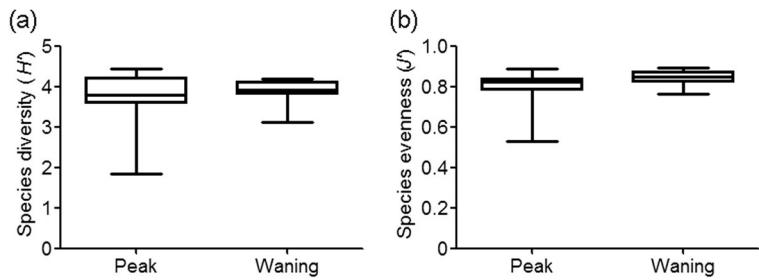
(51.5) compared to the waning phase (58.6) (Table 5). A total of six species were identified as the characterizing species of the peak phase, whereas in the waning phase, the number was 10 (Table 5). The copepod species, *Oithona plumifera*, *Macrosetella gracilis*, *Calanopia minor*, *Acartia danae*, *Centropages furcatus*, and *Urocorycaeus longistylis* were the important discriminating species between the peak and waning phases, and the average dissimilarity value was 52.4 (Table 5).

Correlation

Irrespective of the sampling periods, the interrelation of the zooplankton abundance with the various size-structured phytoplankton biomasses exhibited a positive correlation with the nanophytoplankton (Supplementary Fig. 1). The macrophytoplankton exerted a strong positive influence only in the waning period. Though the microsize class maintained a positive influence on zooplankton abundance during both the sampling phases, the interrelation between the zooplankton and picophytoplankton was observed to be minimum during both the sampling phases (Supplementary Fig. 1).

Redundancy analysis

The interrelation of the zooplankton taxa with other biotic (phytoplankton biomass and abundance) and abiotic variables was displayed in the RDA triplot (Fig. 9). During peak phase, zooplankton biomass and abundance were positively correlated with chlorophyll *a*, phytoplankton abundance, and nutrients especially phosphate and silicate, and in the waning phase, also the scenario remained mostly similar (Fig. 9). During both phases, the taxa Copepoda and Copelata were positively correlated with chlorophyll *a* and the phytoplankton abundance. Fish larvae, which had relatively good abundance in the peak phase, were positively correlated with chlorophyll *a*, and with the abundance of both phytoplankton and Copepoda (Fig. 9). A notable feature observed in the waning phase was the negative interrelation of most of the zooplankton taxa with temperature. The RDA triplots depicted in Fig. 10 delineated the interrelations between the abiotic variables, phytoplankton species, and copepods. Among the abiotic variables, a majority of the copepod species had a negative relation with temperature especially during waning

Fig. 8 k-Dominance plot of the copepod species for both the sampling periods
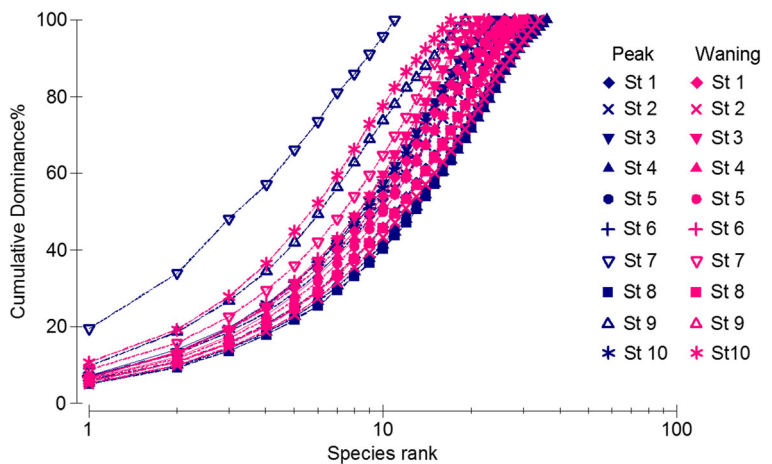
Table 5 (a) Characterizing species of Copepoda during peak and waning phases of El Niño, and (b) discriminating species of Copepoda between two phases

(a)

Species	Av.Abund	Av.Sim	Sim/SD	Contrib%	Cum.%
Peak phase					
Oithona plumifera	2.03	5.24	4.06	10.03	10.03
Bestiolina similis	1.97	4.35	1.81	8.32	18.34
Acrocalanus gracilis	1.68	4.24	4.83	8.1	26.44
Canthocalanus pauper	1.51	3.65	3.06	6.98	33.42
Undinula vulgaris	1.44	3.56	3.47	6.8	40.22
Corycaeus speciosus	1.42	3.2	1.78	6.12	46.34
Waning phase					
Macrosetella gracilis	1.87	5.99	6.36	10.23	10.23
Bestiolina similis	1.67	5.28	6.55	9	19.23
Corycaeus speciosus	1.53	4.76	6.72	8.13	27.37
Oncaea venusta	1.37	4.04	1.86	6.9	34.26
Acrocalanus gracilis	1.3	3.81	1.89	6.5	40.76
Paracalanus aculeatus	1.35	3.65	1.89	6.22	46.98
Calanopia minor	1.29	3.56	1.83	6.07	53.05
Oithona brevicornis	1.17	3.17	1.8	5.42	58.47
Undinula vulgaris	1.04	2.72	1.85	4.64	63.1
Urocorycaeus longistylis	0.94	2.63	1.87	4.48	67.59

(b)

Species	Av.Abund	Av.Abund	Av.Diss	Diss/SD	Contrib%
Oithona plumifera	2.03	0.14	3.08	2.41	5.87
Macrosetella gracilis	0.4	1.87	2.42	3.01	4.61
Calanopia minor	0.16	1.29	2.06	1.99	3.93
Acartia danae	1.11	0.34	1.44	1.75	2.75
Centropages furcatus	1.02	0.43	1.31	1.50	2.49
Urocorycaeus longistylis	0.48	0.94	1.3	1.87	2.48

phase (Fig. 10). During the peak phase of El Niño, the calanoid copepods like *Canthocalanus pauper*, *Undinula vulgaris*, *Acrocalanus gracilis*, and the cyclopoid copepod *Oithona plumifera* were positively correlated with the *Diploneis* sp., *Fragilaria crotonensis*, *Pleurosigma* sp., *Prorocentrum compressum*, and *Protoperidinium* sp. (Fig. 10). The copepod, *Bestiolina similis*, *Paracalanus aculeatus*, and *Corycaeous* spp. had a positive affinity to the diatoms *Navicula delicatula* and *Odontella mobiliensis*. The carnivorous copepod, *Oncaea venusta,* was positively correlated with herbivorous copepods, *Bestiolina simils* and *Paracalanus aculeatus* (Fig. 10). The copepod endemic to Lakshadweep, *Acartia dweepi*, had a strong positive affinity with temperature, salinity, and the dinoflagellate *Prorocentrum lima* (Fig. 10).

In the waning phase, the harpacticoid copepod, *Macrosetella gracilis*, was strongly correlated with the blue-green algae, *Trichodesmium erythraeum* (Fig. 10).

Discussion

The conceptual framework is beyond doubt that shifts in the rainfall patterns during El Niño leads to atmospheric teleconnections, that is, changes in the wind circulation affect patterns of weather variability worldwide (Trenberth et al. 1998; McPhaden 2004). However, the teleconnections vary based on the amplitude of the SST anomaly (McPhaden et al. 2006), and in the Indian Ocean, the resultant effect is complex due to its
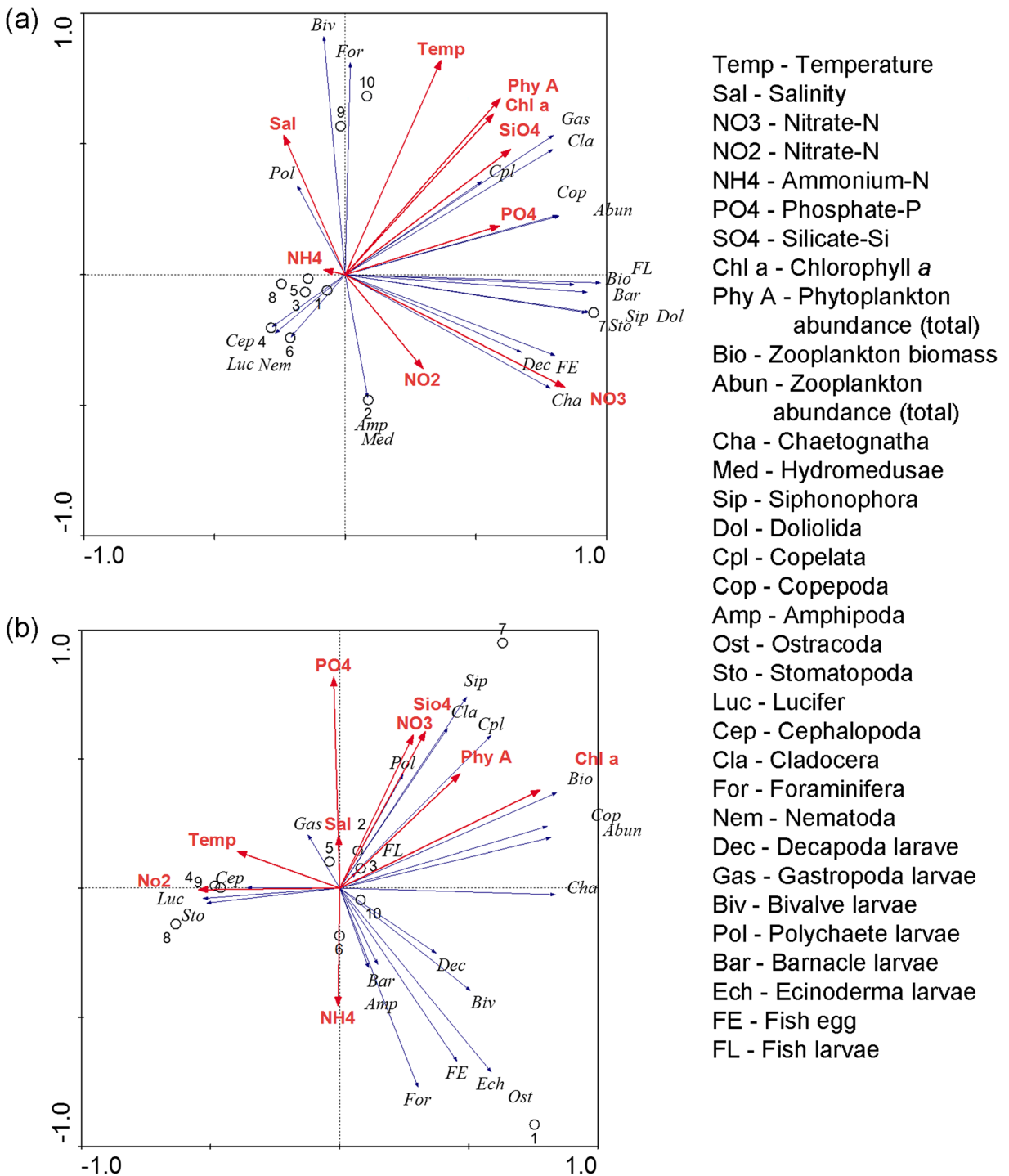
Temp - Temperature
Sal - Salinity
NO3 - Nitrate-N
NO2 - Nitrate-N
NH4 - Ammonium-N
PO4 - Phosphate-P
SO4 - Silicate-Si
Chl a - Chlorophyll *a*
Phy A - Phytoplankton
       abundance (total)
Bio - Zooplankton biomass
Abun - Zooplankton
       abundance (total)
Cha - Chaetognatha
Med - Hydromedusae
Sip - Siphonophora
Dol - Doliolida
Cpl - Copelata
Cop - Copepoda
Amp - Amphipoda
Ost - Ostracoda
Sto - Stomatopoda
Luc - Lucifer
Cep - Cephalopoda
Cla - Cladocera
For - Foraminifera
Nem - Nematoda
Dec - Decapoda larave
Gas - Gastropoda larvae
Biv - Bivalve larvae
Pol - Polychaete larvae
Bar - Barnacle larvae
Ech - Ecinoderma larvae
FE - Fish egg
FL - Fish larvae

Fig. 9 RDA triplot showing interrelations between the abiotic variables and zooplankton taxa during **a** peak and **b** waning phases

interaction with the Indian Ocean Dipole (Luo et al. 2010). Hence, a ground truth evidence for the SST anomaly in this region of Indian Ocean was analyzed for the present ENSO cycle (2010–2016) and the observed positive SST anomaly during the present year (2015–2016) signifies the effect of El Niño on this part of Indian Ocean (Fig. 2). As this current El Niño event is one of the strongest in the last 50 years (https://www.
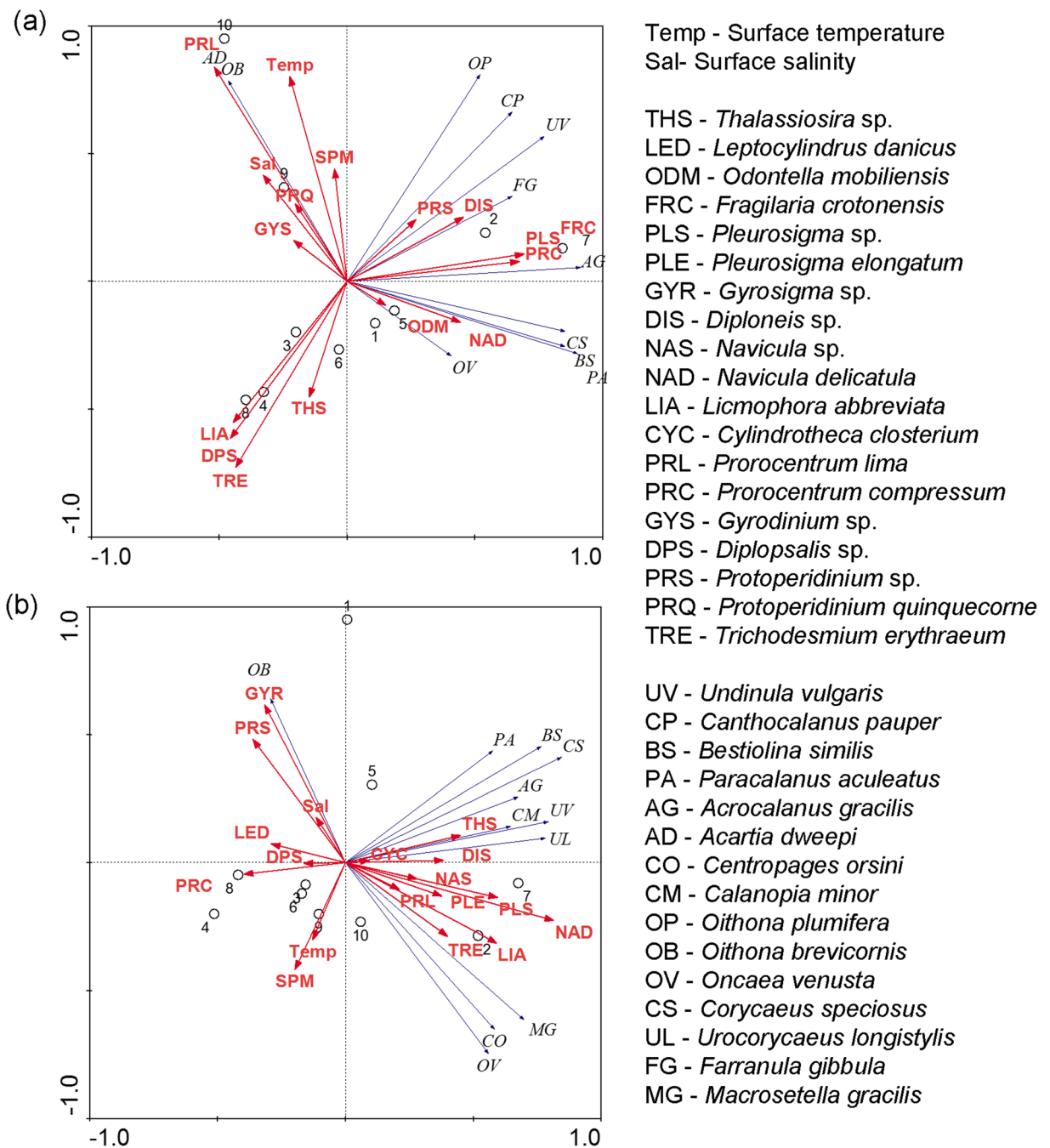
Temp - Surface temperature
Sal - Surface salinity

THS - *Thalassiosira* sp.
LED - *Leptocylindrus danicus*
ODM - *Odontella mobiliensis*
FRC - *Fragilaria crotonensis*
PLS - *Pleurosigma* sp.
PLE - *Pleurosigma elongatum*
GYR - *Gyrosigma* sp.
DIS - *Diploneis* sp.
NAS - *Navicula* sp.
NAD - *Navicula delicatula*
LIA - *Licmophora abbreviata*
CYC - *Cylindrotheca closterium*
PRL - *Prorocentrum lima*
PRC - *Prorocentrum compressum*
GYS - *Gyrodinium* sp.
DPS - *Diplopsalis* sp.
PRS - *Protoperidinium* sp.
PRQ - *Protoperidinium quinquecorne*
TRE - *Trichodesmium erythraeum*

UV - *Undinula vulgaris*
CP - *Canthocalanus pauper*
BS - *Bestiolina similis*
PA - *Paracalanus aculeatus*
AG - *Acrocalanus gracilis*
AD - *Acartia dweepi*
CO - *Centropages orsini*
CM - *Calanopia minor*
OP - *Oithona plumifera*
OB - *Oithona brevicornis*
OV - *Oncaea venusta*
CS - *Corycaeus speciosus*
UL - *Urocorycaeus longistylis*
FG - *Farranula gibbula*
MG - *Macrosetella gracilis*

Fig. 10 The interrelation between the abiotic variables, phytoplankton species, and copepods during **a** peak and **b** waning phases

), the strong teleconnections might have induced remarkable variability in the SST of the Lakshadweep Sea surrounding the Lakshadweep group of islands. The observed higher in situ temperature in the waning phase compared to that in the peak phase might have happened by the combined effect of both El Niño and the seasonal impact. In general, monsoons have a strong influence in regulating the climatology of the tropical northern Indian Ocean and the SST during February–

March (winter monsoon) period is generally less than that observed during May (spring intermonsoon, Shenoi et al. 1999). Thus, the relatively high SST during the waning period (last week of May 2016) compared to the peak period (first week of March 2016) in both in situ and satellite observations might be the resultant effect of this seasonal intervention in the temperature distribution.

The increase in the percentage contribution of dead and weak corals as a result of the severe bleaching affecting more than 60% of the live corals indicates the severe impact of the El Niño 2015–2016 on the coral community of the reef ecosystem. The observed "whitening of corals" or the coral bleaching is often accounted as a stress response of the coral species in which they turn white or pale white due to the expulsion of the intracellular symbionts or zooxanthellae upon the unprecedented rise in SST associated with climatic events or global warming. Recent reports on the El Niño-induced mass bleaching incidents in the Great Barrier Reef of the Pacific Ocean authenticate the global impact of this atmospheric event on the coral reef ecosystems worldwide (http://www.gbrmpa.gov.au/media-room/coral-bleaching). The detail information of Eakin 2016 also shows the impact of El Niño 2015–2016 on the coral community. Hence, considering the intensity of the El Niño 2015 (Chen et al. 2016) along with the persistent positive SST anomaly observed throughout the year in the Lakshadweep Sea region, mass bleaching seems to be a much-anticipated incident whose severity is determined by the duration of the higher SST in this region.

In contrast to the productive upwelling zones characterized by higher nutrient concentrations (Kämpf and Chapman 2016), the coral reef ecosystems, despite being the most productive and diverse ecosystem, are renowned for their oligotrophic nature (de Goeij et al. 2013). Thus, the oligotrophic environment witnessed in the reef environment during both the sampling phases in our study substantiates the view on the trophic status of reef ecosystems in the global ocean. In the waning phase, a significant drop was observed in the concentration of all the major nutrients in the study region (Fig. 4). In general, the advection of offshore water plays a prime role in the nutrient replenishment process in reef ecosystems (Hancock et al. 2006). For this, the concentration of nutrients in the source water is crucial for enhancing the nutrient status, and hence, the oligotrophic condition reported earlier for the Lakshadweep Sea in

the vicinity of the coral islands during the study period (Sengupta et al. 1979) might have a negligible role in the nutrient enhancement process of the reef ecosystem. Nutrient enrichment in conjunction with the physical process like upwelling is also known to augment the nutrient levels of the reef ecosystem. However, as upwelling is reported to occur in conjunction with the summer monsoon (June–September) (Muraleedharan and Prasannakumar 1996), its contribution to the nutrient enrichment process of the reef waters during the study period gets invalidated. Thus, the bioavailable nutrients in the oceanic waters might have gradually been utilized by the biotic community and subsequently led to the significant drop in the concentration in the waning phase.

The nutrient status of an environment often provides the conceptual explanation of the nature of the productivity and the phytoplankton functional group and community structure in the reef ecosystem (Sommer 2000). The lower nutrient concentration during the waning phase might have been transformed into the lower chlorophyll a as the phytoplankton biomass and abundance is primarily controlled by the availability of nutrients (Hecky and Kilham 1988). Though diatoms were abundant during both phases, their abundance was ~ 2 times higher in the peak phase. Diatoms are an ecologically diverse phytoplankton community and are known to flourish in all aquatic systems due to their well refined cellular processes for the efficient acquisition of nutrients and sunlight (Seckbach and Kociolek 2011). However, their growth and proliferation rely greatly on the sufficient supply of bioavailable inorganic nitrogen, phosphorus, silicon, and trace elements (Armbrust 2009). Hence, the markedly lower concentration of all the major nutrients in the waning phase might have restricted their abundances in the reef ecosystem (Karati et al. 2017). An interesting feature observed during the study was the predominance of the blue-green algae, *Trichodesmium erythraeum*, in the waning phase when all the nutrients were found to be in the trace concentrations. In the nutrient-depleted ecosystem, *Trichodesmium*, the non-heterocystous filamentous blue-green algae is known to play a significant role in fixing atmospheric nitrogen (Carpenter and Price 1977; Bergman et al. 2013), and hence, the lower nitrate concentration observed in the waning phase might not have affected the proliferation of this diazotroph in the Kavaratti reef waters. Furthermore, their unique capability to utilize the dissolved organic

phosphorous (not analyzed in the present study) in the water column along with the dissolved inorganic phosphorous (Sohm and Capone 2006) might have also supported their higher proliferation in the waning phase.

The variations brought about by the El Niño in the physiological status of reef corals and also in the phytoplankton community structure were found to have a marked influence on the abundance and distribution of the zooplankton community of the reef ecosystem. The observed negative relation of the most of the zooplankton taxa with temperature in the waning phase indicates towards their less preference for the higher SST associated with the El Niño (Fig. 9). The positive relation between the phytoplankton and zooplankton (both biomass and abundance) evident in the RDA analysis signifies the vital role played by the phytoplankton in the sustenance of the reef zooplankton community. The lower biomass and abundance of the zooplankton community in the waning phase of El Niño might be the effect of the significant drop in the abundance of the primary producer community. Despite the prominent temporal variation witnessed in the zooplankton biomass and abundance in reef ecosystem, higher zooplankton abundance was always observed in the sampling locations predominated by the live coral community. Though the mutualistic associations with the microscopic intracellular algal symbionts are known to provide the corals with a majority of their nutritional requirements, corals generally rely greatly on the zooplankton community for their essential amino acids, vitamins, mineral, and nitrogenous requirements critical for their tissue growth and reproductive processes (Houlbrèque et al. 2004). Hence, the higher abundance of zooplankton in the live coral region appeared as a paradox which could only be better explained by the predator avoidance strategy by seeking shelter between the coral branches and crevices. The Kavaratti reef is known as an abode of a diverse coral reef fish community represented by 27 families and 65 species of which majority of the species are considered omnivorous in their dietary habit (Vijay Anand and Pillai 2007). Hence, the reef zooplankton might have utilized the coral structures as a potential hideout from the predators, in particular from the reef fishes thus resulting in their enhanced abundance in regions having good coral cover compared to the regions with the sandy substratum. Moreover, studies pertaining to the coral mucous being a potential energy source of reef zooplankton (Gerber and Gerber

1979; Gottfried and Roman 1983) further authenticate the higher zooplankton incidence near the corals. Corals are known to secrete a high-energy complex polysaccharide-protein-lipid mucous material as a protective physicochemical barrier against a wide variety of environmental stresses (Brown and Bythell 2005). The mucopolysaccharide matrix of the coral mucus mostly contains high-energy compounds such as fatty acids, triglycerides, and wax esters (Coles and Strathmann 1973; Ducklow and Mitchell 1979). Hence, the higher incidence of the primarily heterotrophic zooplankton community, at regions of healthy corals, can be attributed to a strategy for the utilization of coral mucous as an important food source (Richman et al. 1975; Gottfried and Roman 1983). However, the heterogeneity in the abundance of the zooplankton community in the study region between regions having coral cover and sandy substratum was more conspicuous during the peak El Niño phase compared to the waning period. As the production and composition of mucous vary greatly according to the health of corals, the remarkable bleaching and mortality of the coral community in the waning phase subsequent to the El Niño event might have reduced mucus production and in turn resulted in a relatively homogenous zooplankton distribution pattern in the study region.

The decline in the abundance of many carnivorous zooplankton taxa specifically in the waning phase might have been stemmed by the lower abundance of their most preferred prey item, Copepoda, in the study region. The positive relation identified between the fish larvae and both phytoplankton and zooplankton abundances indicates towards their omnivorous dietary habits. Studies of Vijay Anand and Pillai (2007) suggesting the omnivorous diet preferences of the majority of the reef fishes of the Kavaratti atoll further substantiate the above observation. The concomitant decline in fish larval abundance with the drop in phytoplankton and Copepoda population in the waning phase points to the less productive environment constraining the reproductive success and population growth of reef fishes and ultimately leading to the reduced fishery potential of the ecosystem (Glynn 1988). Moreover, fishes are considered to thrive well within a specific range of environmental conditions favorable for their growth and reproduction and any deviations from their acclimatized environment especially in the temperature may have a potential impact on their survival and reproductive rates (Barton et al. 2002). Hence, the negative relation

observed between the temperature and ichthyoplankton in the waning period suggests towards the impact of higher SST on their breeding and recruitment. Thus, the variability in the status of the reef health in terms of the water chemistry, nutrient concentration, phytoplankton abundance, and community composition between the peak and waning phases led towards discernible changes in both community composition and the abundances of the zooplankton taxa resulting into the significantly distinguishable community structures (global $R = 0.395$, $P = 0.001$) between the two periods.

Although the abundance of the dominant zooplankton Copepoda decreased in accordance with the phytoplankton abundance during the waning phase, a detailed study of their spatiotemporal distribution and diversity pattern was a prerequisite to reveal the adaptability of the copepod community, as in any ecosystem, the diverse species characterized by specific traits responds differently in the effective functioning of an ecosystem (Lefcheck et al. 2015). Thus, the observed variation in the copepod community composition, abundance, and percentage contribution between the two sampling periods might have happened by the differential responses of the diverse copepod species towards the varied physicochemical and biotic scenario in the reef environment during the two phases of the El Niño event. During the peak period, the positive interrelation of the diatoms (*Diploneis* sp., *Fragilaria crotonensis*, *Pleurosigma* sp.) and the calanoids (*Canthocalanus pauper*, *Undinula vulgaris*, *Acrocalanus gracilis*) indicates the vital trophic link existing between them (Fig. 10).

In contrast to the higher abundance of the majority of copepods belonging to the orders Calanoida and Poecilostomatoida in the peak phase, most of the copepod species belonging to Harpacticoida exhibited increased abundance in the waning period. Many pelagic harpacticoid species are known to utilize the diazotroph, *Trichodesmium*, as their nutritional source (O'Neil and Roman 1994), and the predominance of this diazotroph in the nutrient-poor environment during the waning phase might have helped in the sustenance of their population. Among the harpacticoids, the increase in abundance during waning phase was most prominent in *Macrosetella gracilis*, as this species is best known to effectively utilize the *Trichodesmium* both as a physical substrate and as a potential food source (Björnberg 1965; O'Neil 1998). Most of the calanoids and poecilostomatoids avoid this diazotroph as a food source due to the slight toxicity which is proven to have

a lethal effect on them (O'Neil and Roman 1994). However, *Macrosetella gracilis* is considered to be resistant to this toxin and needs only less energy expenditure for the detoxification process and hence can effectively graze upon them as a dietary resource. Also, the use of *Trichodesmium* as a "skate" often increases their mate encounter chances, which again is very much crucial for the regulation of their population dynamics (Björnberg 1965). The attachment of eggs and hatched nauplii by *M. gracilis* to the floating *Trichodesmium* mats are known to provide them more protection and nutritional requirements and thus often act as a better nursery ground for the developing stages (O'Neil 1998; Eberl et al. 2007). These benefits might have resulted in the strong positive correlation observed between the abundance of *M. gracilis* with *Trichodesmium* (Fig. 10) in the study region. A similar observation in oligotrophic reef ecosystems of the Red Sea (Böttger-Schnack and Schnack 1989) substantiates the above view. The notable positive correlation observed between the zooplankton and the macrophytoplankton biomass in the waning phase might have happened due to the association between the copepod, *M. gracilis*, and phytoplankton, *Trichodesmium erythraeum*. The size of *Trichodesmium erythraeum* is usually > 200 μM (Fig. 2 in Bergman et al. 2013), and also due to their colonial nature, there is a definite possibility of this phytoplankton contributing a prominent share of the macrophytoplankton biomass in the study region.

Another noteworthy feature observed during the study was the predominance of *Acartia dweepi*, an endemic copepod of the Lakshadweep atolls (Haridas and Madhupratap 1977) in the sandy substratum (stations 7 and 9) in concurrence with the dinoflagellate, *Prorocentrum lima*, during the peak phase of El Niño. *P. lima* is a primarily benthic dinoflagellate common in tropical and temperate waters. Generally, found in epiphytic association with the seagrass community in coral reef ecosystem (Forden et al. 2005), these species are also known to behave as a tachyplankton in environments characterized with the sandy substratum. Being a toxic algae known to produce both intra- and extracellular toxins (okadaic acid, dinophysistoxin and their derivatives) (Morton and Tindall 1995; Bravo et al. 2001), the reduced palatability of this toxic dinoflagellate to majority of the copepod species might have contributed to the lower abundance of the other copepod grazers in sampling locations where this dinoflagellate dominated. Though a detailed dietary evaluation of *A. dweepi* was

not carried out, it is assumed that this copepod species might be either resistant to the toxin produced by *P. lima* or might have dominated at stations 7 and 9 where there was less competitive pressure from the other grazing copepod species.

The difference in the position of the sampling locations between the peak phases and waning phases in the MDS plot might have happened due to the variation observed in the copepod abundance and community structure between the two sampling phases. The discriminating species identified through SIMPER played a determining role in maintaining the discreteness in the copepod community structure of the two sampling periods. The significantly distinguishable community structure (global $R = 0.405$, $P = 0.001$) of the two periods might have happened by the resultant effect of the species-specific responses towards the varied physicochemical and biotic scenario in the reef ecosystem with the progression of El Niño from its peak to waning phase.

Although the overall species diversity in the reef ecosystem along two periods did not exhibit significant variation in both H' (av. 3.72 ± 0.75 and 3.89 ± 0.33 during peak and waning phases, respectively) and J' (av. 0.79 ± 0.1 and 0.84 ± 0.03 during peak and waning phases, respectively), the spatial analysis helped to identify the discrete nature between two sampling periods. The varied nature of substratum (live coral and sandy) and the spatiotemporal variability in phytoplankton community structure have led to pronounced variability in the copepod diversity pattern during peak phase (both minimum and maximum diversities during this period) (Fig. 7). On the contrary, when the corals were severely bleached and when a nutrient impoverished environment prevailed in the reef waters with a marked predominance of the diazotrophic cyanobacterium, *Trichodesmium* in all the sampling locations, the relatively homogenous condition resulted in less variation in the copepod diversity in the waning phase. Thus, the differential response of the copepod species towards the changing abiotic and biotic nature of the El Niño-induced ecosystem, in turn, influenced the structure and function of the reef ecosystem.

Conclusion

The monthly mean SST of the Lakshadweep Sea around the coral atolls exhibited a positive anomaly during the current El Niño year (2015–2016), and the observed higher SST in the lagoon affected the reef ecology. The changes in the hydrography, variability in size-structured phytoplankton biomass and community structure, and the decline in the coral health had a significant effect on both zooplankton abundance and community structures. The drop in the zooplankton abundance during the waning phase was in accordance with the decline in phytoplankton abundance during this period, and this variation was more prominent in the locations with coral cover than with sandy bottom. The dominant zooplankton taxon Copepoda also experienced a significant change in their abundance and population structure between the peak phase and waning phases. The harpacticoid, *Macrosetella gracilis*, had an important role in the copepod community dynamics during the waning phase. Their capability to effectively utilize the cyanobacterium, *Trichodesmium erythraeum*, both as a physical substrate and as a potential food source enabled them to increase their population in the waning phase when the abundances of calanoids and poecilostomatoids were less. The study first time depicting the detailed responses of the zooplankton community towards the El Niño-affected reef ecosystem in the Indian Ocean will be helpful in understanding the sensitive reef ecology in similar environments worldwide.

References

Achuthankutty, C. T., Nair, S. R., Haridas, P., & Madhupratap, M. (1989). Zooplankton composition of the Kalpeni and Agatti atolls, Lakshadweep archipelago. *Indian Journal of Marine Science, 18*, 151–154.

Armbrust, E. V. (2009). The life of diatoms in the world's oceans. *Nature, 459*, 185–192.

Arthur, R. (2000). Coral bleaching and mortality in three Indian reef regions during an El Niño southern oscillation event. *Current Science, 79*, 1723–1729.

Baker, A. C., Glynn, P. W., & Riegl, B. (2008). Climate change and coral reef bleaching: an ecological assessment of long-term impacts, recovery trends and future outlook. *Estuarine Coastal and Shelf Science, 80*, 435–471.

Bakun, A., & Broad, K. (2003). Environmental 'loopholes' and fish population dynamics: comparative pattern recognition with focus on El Nino effects in the Pacific. *Fisheries Oceanography, 12*, 458–473.

Barton, B. A., Morgan, J. D., Vijayan, M. M., & Adams, S. M. (2002). Physiological and condition-related indicators of environmental stress in fish. In S. M. Adams (Ed.), *Biological indicators of aquatic ecosystem stress* (pp. 111–148). Bethesda: American Fisheries Society.

Bergman, B., Sandh, G., Lin, S., Larsson, J., & Carpenter, E. J. (2013). *Trichodesmium*—a widespread marine cyanobacterium with unusual nitrogen fixation properties. *FEMS Microbiology Reviews, 37*, 286–302.

Björnberg, T. K. S. (1965). Observations on the development and the biology of the Miracidae Dana (Copepoda: Crustacea). *Bulletin of Marine Science, 15*, 512–520.

Böttger-Schnack, R., & Schnack, D. (1989). Vertical distribution and population structure of *Macrosetella gracilis* (Copepoda: Harpacticoida) in the Red Sea in relation to the occurrence of *Oscillatoria* (*Trichodesmium*) spp (Cyanobacteria). *Marine Ecology Progress Series, 52*, 17–31.

Bravo, I., Fernandez, M. L., & Martinez, R. A. (2001). Toxin composition of the toxic dinoflagellate *Prorocentrum lima* isolated from different locations along the Galician coast (NW Spain). *Toxicon, 39*, 1537–1545.

Brown, B. E., & Bythell, J. C. (2005). Perspectives on mucus secretion in reef corals. *Marine Ecology Progress Series, 296*, 291–309.

Carpenter, E. J., & Price, C. C. (1977). Nitrogen fixation, distribution, and production of *Oscillatoria* (*Trichodesmium*) spp. in the western Sargasso and Caribbean Seas. *Limnology and Oceanography, 22*, 60–72.

Chen, S., Wu, R., Chen, W., Yu, B., & Cao, X. (2016). Genesis of westerly wind bursts over the equatorial western Pacific during the onset of the strong 2015–2016 El Niño. *Atmospheric Science Letters, 17*, 384–391.

Claar, D. C., Szostek, L., McDevitt-Irwin, J. M., Schanze, J. J., & Baum, J. K. (2018). Global patterns and impacts of El Niño events on coral reefs: a meta-analysis. *PLoS One, 13*(2), e0190957.

Clarke, K. R., & Gorley, R. N. (2015). *PRIMER v7: user manual/tutorial*. Plymouth: PRIMER-E.

Clifford, H. T., & Stephensen, W. (1975). *An introduction to numerical classification*. New York: Academic Press.

Coles, S. L., & Strathmann, R. (1973). Observations on coral mucus "flocs" and their potential trophic significance. *Limnology and Oceanography, 18*, 673–678.

Conway, D. V. P., White, R. G., Hugues-Dit-Ciles, J., Gallienne, C. P., & Robins, D. B. (2003). *Guide to the coastal and surface zooplankton of the South-Western Indian Ocean*. Plymouth: Marine Biological Association of the United Kingdom.

Costello, M. J., & Chaudhary, C. (2017). Marine biodiversity, biogeography, deep-sea gradients, and conservation. *Current Biology, 27*, R511–R527.

De Goeij, J. M., Van Oevelen, D., Vermeij, M. J., Osinga, R., Middelburg, J. J., de Goeij, A. F., & Admiraal, W. (2013). Surviving in a marine desert: the sponge loop retains resources within coral reefs. *Science, 342*, 108–110.

Diaz-Pulido, G., McCook, L. J., Dove, S., Berkelmans, R., Roff, G., Kline, D. I., Weeks, S., Evans, R. D., Williamson, D. H.,

& Hoegh-Guldberg, O. (2009). Doom and boom on a resilient reef: climate change, algal overgrowth and coral recovery. *PLoS One, 4*(4), e5239.

Ducklow, H. W., & Mitchell, R. (1979). Composition of mucus released by coral reef coelenterates. *Limnology and Oceanography, 24*, 706–714.

Eakin, M. (2016). Outlook on coral bleaching: El Niño, the guest overstaying his welcome. Presentation in 35 Meeting Washington DC, February, 2016. https://www.coralreef.gov/meeting35/pdf/7_2016_Outlook_on_Coral_Bleaching.

Eberl, R., Cohen, S., Cipriano, F., & Carpenter, E. J. (2007). Genetic diversity of the pelagic harpacticoid copepod *Macrosetella gracilis* on colonies of the cyanobacterium *Trichodesmium* spp. *Aquatic Biology, 1*, 33–43.

Edwards, M., & Richardson, A. J. (2004). Impact of climate change on marine pelagic phenology and trophic mismatch. *Nature, 430*, 881–884.

Gerber, R., & Gerber, M. (1979). Ingestion of natural particulate organic matter and subsequent assimilation, respiration and growth by tropical lagoon zooplankton. *Marine Biology, 52*, 33–43.

Glynn, P. W. (1988). El Niño-Southern Oscillation 1982-1983: nearshore population, community, and ecosystem responses. *Annual Review of Ecology Evolution and Systematics, 19*, 309–346.

Glynn, P. W., Mones, A. B., Podestá, G. P., Colbert, A., & Colgan, M. W. (2017). El Niño-Southern Oscillation: Effects on Eastern Pacific coral reefs and associated biota. In P. W. Glynn, D. P. Manzello, & I. C. Enochs (Eds.), *Coral reefs of the Eastern Tropical Pacific* (pp. 251–290). Netherlands: Springer.

Gottfried, M., & Roman, M. R. (1983). Ingestion and incorporation of coral-mucus detritus by reef zooplankton. *Marine Biology, 72*, 211–218.

Grasshoff, K. (1983). Determination of oxygen. In K. Grasshoff, M. Ehrhardt, & K. Kremling (Eds.), *Methods of sea water analysis* (pp. 61–72). Weinheim: Verlag Chemie.

Hagen, W. (2000). Biovolume and biomass determinations. In R. Harris, P. Wiebe, J. Lenz, H. R. Skjoldal, & M. E. Huntley (Eds.), *ICES zooplankton methodology manual* (pp. 87–147). London: Academic Press.

Hancock, G. J., Webster, I., & Stieglitz, T. C. (2006). Horizontal mixing of Great Barrier Reef waters: offshore diffusivity determined from radium isotope distribution. *Journal of Geophysical Research Oceans, 111*, C12019. https://doi.org/10.1029/2006JC003608.

Haridas, P., & Madhupratap, M. (1977). *Acartia dweepi*, a new species of copepod (Acartidae, galanoida) from Lakshadweep. *Current Science, 47*, 176–177.

Harris, R., Wiebe, P., Lenz, J., Skjoldal, H. R., & Huntley, M. E. (Eds.). (2000). *ICES zooplankton methodology manual*. London: Academic Press.

Hays, G. C., Richardson, A. J., & Robinson, C. (2005). Climate change and marine plankton. *Trends in Ecology and Evolution, 20*, 337–344.

Hecky, R. E., & Kilham, P. (1988). Nutrient limitation of phytoplankton in freshwater and marine environments: a review of recent evidence on the effects of enrichment. *Limnology and Oceanography, 33*, 796–822.

Heidelberg, K. B., O'Neil, K. L., Bythell, J. C., & Sebens, K. P. (2010). Vertical distribution and diel patterns of zooplankton

abundance and biomass at Conch Reef, Florida Keys (USA). *Journal of Plankton Research, 32*, 75–91.

Houlbrèque, F., Tambutté, E., Allemand, D., & Ferrier-Pagès, C. (2004). Interactions between zooplankton feeding, photosynthesis and skeletal growth in the scleractinian coral *Stylophora pistillata. Journal of Experimental Biology, 207*, 1461–1469.

James, P. S. B. R. (2011). The Lakshadweep: islands of ecological fragility, environmental sensitivity and anthropogenic vulnerability. *Journal of Coastal Environment, 2*, 9–25.

Kämpf, J., & Chapman, P. (2016). *Upwelling systems of the world. A scientific journey to the most productive marine ecosystem.* Switzerland: Springer.

Karati, K. K., Vineetha, G., Madhu, N. V., Anil, P., Dayana, M., Shihab, B. K., Muhsin, A. I., Riyas, C., & Raveendran, T. V. (2017). Variability in the phytoplankton community of Kavaratti reef ecosystem (northern Indian Ocean) during peak and waning periods of El Niño 2016. *Environmental Monitoring and Assessment, 189*, 1–17.

Kelley, R. (2009). Indo Pacific coral finder. See www.byoguides.com.

Lefcheck, J. S., Byrnes, J. E., Isbell, F., et al. (2015). Biodiversity enhances ecosystem multifunctionality across trophic levels and habitats. *Nature Communications, 6*, 1–7.

Luo, J. J., Zhang, R., Behera, S. K., Masumoto, Y., Jin, F. F., Lukas, R., & Yamagata, T. (2010). Interaction between El Nino and extreme Indian ocean dipole. *Journal of Climate, 23*, 726–742.

Madhupratap, M., Achuthankutty, C. T., & Nair, S. S. (1991). Zooplankton of the lagoons of the Laccadives: diel patterns and emergence. *Journal of Plankton Research, 13*, 947–958.

McPhaden, M. J. (2004). Evolution of the 2002/03 El Niño. *Bulletin of the American Meteorological Society, 85*, 677–695.

McPhaden, M. J., Zebiak, S. E., & Glantz, M. H. (2006). ENSO as an integrating concept in earth science. *Science, 314*, 1740–1745.

Morton, S. L., & Tindall, D. R. (1995). Morphological and biochemical variability of the toxic dinoflagellate *Prorocentrum lima* isolated from three locations at Heron Island, Australia. *Journal of Phycology, 31*, 914–921.

Muraleedharan, P. M., & Prasannakumar, S. (1996). Arabian Sea upwelling—a comparison between coastal and open ocean regions. *Current Science, 71*, 842–846.

O'Neil, J. M. (1998). The colonial cyanobacterium *Trichodesmium* as a physical and nutritional substrate for the harpacticoid copepod *Macrosetella gracilis. Journal of Plankton Research, 20*, 43–59.

O'Neil, J. M., & Roman, M. R. (1994). Ingestion of the cyanobacterium *Trichodesmium* spp. by pelagic harpacticoid copepods *Macrosetella, Miracia* and *Oculosetella. Hydrobiologia, 292*, 235–240.

Richardson, A. J. (2008). In hot water: zooplankton and climate change. *ICES Journal of Marine Science, 65*, 279–295.

Richman, S., Loya, Y., & Sloboclkin, L. B. (1975). The rate of mucus production by corals and its assimilation by the coral

reef copepod *Acartia negligens. Limnology and Oceanography, 20*, 918–923.

Seckbach, J., & Kociolek, J. P. (Eds.). (2011). *The diatom world.* New York: Springer.

SenGupta, R., Mores, C., Kureishy, T. W., Sankaranarayanan, V. N., Jana, T. K., Naqvi, S. W. A., & Rajagopal, M. D. (1979). Chemical oceanography of the Arabian Sea: part IV—Laccadive Sea. *Indian Journal of Geo-Marine Sciences, 8*, 215–221.

Sewell, R. B. S. (1999). *The copepod of Indian seas.* India: Daya Books.

Shenoi, S. S. C., Shankar, D., & Shetye, S. R. (1999). On the sea surface temperature high in the Lakshadweep Sea before the onset of the southwest monsoon. *Journal of Geophysical Research Oceans, 104*(C7), 15703–15712.

Sohm, J. A., & Capone, D. G. (2006). Phosphorus dynamics of the tropical and subtropical North Atlantic: *Trichodesmium* spp. versus bulk plankton. *Marine Ecology Progress Series, 317*, 21–28.

Sommer, U. (2000). Scarcity of medium-sized phytoplankton in the northern Red Sea explained by strong bottom-up and weak top-down control. *Marine Ecology Progress Series, 197*, 19–25.

Stramma, L., Fischer, T., Grundle, D. S., Krahmann, G., Bange, H. W., & Marandino, C. A. (2016). Observed El Niño conditions in the eastern tropical Pacific in October 2015. *Ocean Science, 12*, 861–873.

Tomas, C. R. (1997). *Identifying marine phytoplankton.* New York: Academic Press.

Trenberth, K. E., Branstator, G. W., Karoly, D., Kumar, A., Lau, N. C., & Ropelewski, C. (1998). Progress during TOGA in understanding and modeling global teleconnections associated with tropical sea surface temperatures. *Journal of Geophysical Research Oceans, 103*(C7), 14291–14324.

Van den Wollenberg, A. L. (1977). Redundancy analysis. An alternative for canonical correlation analysis. *Psychometrika, 42*, 207–219.

Vijay Anand, P. E., & Pillai, N. G. K. (2007). Coral reef fish abundance and diversity of seagrass beds in Kavaratti atoll, Lakshadweep, India. *Indian Journal of Fisheries, 54*, 11–20.

Walther, G. R., Post, E., Convey, P., Menzel, A., Parmesan, C., Beebee, T. J., Fromentin, J. M., Hoegh-Guldberg, O., & Bairlein, F. (2002). Ecological responses to recent climate change. *Nature, 416*, 389–395.

Warwick, R. M., Clarke, K. R., & Somerfield, P. J. (2008). k-Dominance curves. In S. E. Jørgensen & B. D. Fath (Eds.), *Ecological indicators. 3, encyclopedia of ecology, 5* (pp. 2055–2057). Oxford: Elsevier.

Wilson, S. G., Taylor, J. G., & Pearce, A. F. (2001). The seasonal aggregation of whale sharks at Ningaloo Reef, Western Australia: currents, migrations and the El Nino/Southern Oscillation. *Environmental Biology of Fishes, 61*, 1–11.